

Adsorption studies of chromium (VI) on weak base resins Tulsion A-10X (MP) and Amberlyst A-21 (MP) in aqueous and mixed media

Janhavi M. Karekar, Sanjaykumar V. Divekar*

Department of Chemistry, KLS's Gogte Institute of Technology, Affiliated and Autonomous Institution under Visvesvaraya Technological University, Belagavi – 590008, Karnataka, India, Tel. +91 9480398575, Fax +91 831 2441909, email: vmkarekar@git.edu (J.M. Karekar), Tel.+91 988660316, email: svdivekar@git.edu (S.V. Divekar)

Received 8 December 2016; Accepted 29 May 2017

ABSTRACT

The adsorption studies of chromium (VI) in aqueous and aqueous-organic solvents mixed media is carried out using weak base anion exchangers Tulsion A-10 X (MP) and Amberlyst A-21 (MP) by batch process. Adsorption of chromium (VI) is investigated by varying contact time, chromium (VI) concentration, resin dosage, temperature and pH. The effect of solvent on adsorption of chromium (VI) was also studied at different solvent compositions. The percentage of chromium (VI) removal was found faster on Amberlyst A-21 (MP) than Tulsion A-10X (MP) due to the difference in resin structure. However, the percentage removal of chromium (VI) is up to 99% on both the resins. Chromium (VI) removal is maximum in the pH range 2.0 to 5.0 with a resin dosage of 150 mg and initial chromium (VI) concentration 350 mg·L⁻¹. The equilibrium sorption data was analysed with Freundlich and Langmuir isotherms. The data fits well in Langmuir model indicating monolayer adsorption of chromium (VI) on the resin. Adsorption process follows pseudo-second order kinetic equation and is controlled by intra-particle diffusion. The desorption study indicates that NaOH is better desorbent for resin Amberlyst A-21(MP) than Tulsion A-10X(MP). Thermodynamic parameters were evaluated by applying Van't Hoff equation to the adsorption process.

Keywords: Chromium(VI); Anion exchanger; Adsorption isotherm; Kinetics; Equilibrium

1. Introduction

With the rapid growth in industries and urbanization heavy metals are discharged into rivers and other water bodies. Elimination of heavy metals from wastewater from industries is of prime importance to reduce contamination of water bodies. Chromium is one among them which is released from electroplating, metal finishing, mining, leather tanning and textile dyeing industries. The two stable oxidation states of Chromium are Cr(III) and Cr(VI) and between these two forms Cr(VI) is toxic, mutagenic and carcinogenic. Cr(VI) exists in different forms which depends on the pH of the medium, as acid chromate (HCrO₄⁻), chromate (CrO₄²⁻), and dichromate (Cr₂O₇²⁻) [1]. The maximum permissible limit for Cr(VI) in waste water is below 0.01 mg L⁻¹ and 5 mg L⁻¹ for Chromium(III) [2].

The removal of Cr(VI) from the waste water generated from industries can be achieved by several processes, such as coagulation [3], membrane separation [4,5] electro-dialysis [6], electrode-ionization [7] and solvent extraction [8]. However, most of these processes are expensive as they require continuous monitoring and generate toxic sludge which is difficult to dispose [9]. Synthetic ion exchange resins [10–14] have been used by many researchers in recent years. The ion exchange process is found to be more effective among other separation processes due to high selectivity, high mechanical and chemical stability of resins, low cost of regeneration, limited sludge formation and recovery of metals [15].

The present research work emphasizes on adsorption of Cr(VI) from synthetic waste water using two weak base anion exchangers namely Tulsion A-10X(MP) and Amberlyst A-21(MP) having different resin matrix structures and resin fixed ion. Due to weaker physical and chemical stability acrylic resins find fewer applications than styrene divinyl

*Corresponding author.

benzene matrix [15]. In the present research work the efficiency of removal of Cr(VI) using Tulsion A-10X(MP) with acrylic matrix is being compared with Amberlyst A-21(MP) with polystyrene matrix.

To optimize the conditions for the removal of Cr(VI) various parameters such as concentration of Cr(VI), temperature, resin dosage, pH and kinetics of Cr(VI) removal were studied. The equilibrium data generated for the resins, was evaluated by applying various isotherms and kinetic models.

2. Experimental

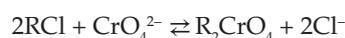
2.1. Materials and methods

A weak base anion exchange resin Tulsion A-10X (MP) was supplied by Thermax Limited, Pune, India as free samples and Amberlyst A-21(MP) was procured from Himedia Laboratories Pvt. Ltd., Mumbai, India. Reconditioning of the resins was done as per the standard procedures and converted into chloride form before carrying out the adsorption study. Table 1 summarizes resin type, matrix structure and capacities of the resins. Aqueous solution containing Cr(VI) was prepared by using $K_2Cr_2O_7$ in double distilled water. The complex forming reagent 1,5-diphenylcarbazide (DPC) and other chemicals used are of analytical reagent grade.

2.1.1. Adsorption studies by batch method

Adsorption studies were carried out with 50 cm³ of potassium dichromate solution and 150 mg of resin in 100 cm³ stoppered volumetric flasks. The flasks are kept for shaking in Toshiba Make thermostat controlled water bath shaker to attain equilibrium at different temperatures 303, 323 and 343 K. Cr(VI) present in the solution phase is analyzed spectrophotometrically by 1,5-diphenyl carbazide method [16] using a UV-visible spectrophotometer Varian Cary 50 Bio at 540 nm.

The ion exchange reaction of Cr(VI) as chromate with chloride ions on the resin phase can be represented as,



in which R represents the resin matrix.

Distribution coefficient (K_d) at equilibrium was calculated using Eq. (1).

$$K_d = \frac{q_e}{C_e} \quad (1)$$

where the amount of metal ion adsorbed on the resin is represented as q_e in mg·g⁻¹ which is calculated by using Eq. (2) and C_e represents the metal ion concentration in solution in mg·L⁻¹ at equilibrium [17].

$$q_e = \frac{V\{C_o - C_e\}}{m} \quad (2)$$

where volume of solution is represented as V in L, weight of resin m in g, and initial and equilibrium concentration of Cr(VI) is represented as C_o and C_e are in mg·L⁻¹ respectively.

Cr(VI) recovery factor was calculated using Eq. (2),

$$\%R = \frac{C_a}{C_o} \times 100 \quad (3)$$

where C_a is the concentration of Cr(VI) adsorbed on the resin and C_o is the initial concentration of Cr(VI) in mg·L⁻¹.

Resin morphology was studied before and after adsorption of Cr(VI) using scanning electron microscope (SEM) and Fourier Transform Infrared Spectroscopy (FT-IR).

Isotherm models Langmuir and Freundlich were applied to the generated data to understand the adsorption process.

2.1.2. Desorption studies

The desorption study was carried out by using different desorbents for reuse of resin. 50 cm³ of Cr(VI) solution of concentration 350 mg·L⁻¹ was kept in contact with 150 mg of resin in Toshiba make mechanical shaker for the period of 2 h. After the adsorption of Cr(VI) on the resin, the resin was washed with double distilled water to remove traces of solution adhered to the resin. The washed resin was treated with 50 cm³ of desorbents like, 1 N NaOH, 1 N HCl and 0.25 N EDTA and kept for shaking for 2 h. After desorption, Cr(VI) concentration in the filtrate was analyzed.

Eq. (4) was used to calculate desorption ratio [18],

$$\text{Desorption ratio} = \frac{\text{Amount of metal ions desorbed}}{\text{Amount of metal ions adsorbed}} \times 100 \quad (4)$$

Table 1
Characteristics of resins

Resin	Tulsion A-10X (MP)	Amberlyst A-21 (MP)
Type	Weak base	Weak base
Matrix structure	Cross linked polyacrylic (Macroporous)	Styrene divinylbenzene (Macroporous)
Functional group	Polyamine	Tertiary amine
Ionic form	Free base form converted to chloride form	Free base form converted to chloride form
Screen size (US mesh)	16–50	22–30
Maximum operating temperature	80°C	100°C
Total capacity in m.eq. /250 mg	0.900	0.720
Moisture content %	52–55%	56–62%

3. Results and discussion

3.1. Effect of the various parameters on adsorption of Cr(VI)

3.1.1. Effect of resin dosage

To study the effect of resin dosage the quantity of resin was varied between 50 mg to 400 mg. The resins were equilibrated with 400 mg·L⁻¹ Cr(VI) solution. Fig. 1 indicates that, the removal of Cr(VI) increases from 55 to 95% for Amberlyst A-21(MP) and from 67 to 97% for Tulsion A-10X(MP) by varying resin dosage from 50 mg to 150 mg. This is mainly because of increase in the available active sites for adsorption. 150 mg of resin dosage is sufficient for the maximum removal of Cr(VI) at concentration 400 mg·L⁻¹.

3.1.2. Effect of pH

The adsorption of Cr(VI) is pH dependent and it is important variable. The effect of pH on adsorption was studied by taking 50 cm³ of Cr(VI) solution of 350 mg·L⁻¹ and 150 mg of resin Tulsion A-10 X (MP) and Amberlyst A-21 (MP) at pH ranging from 1.0 to 9.0. As seen from Fig. 2, around 97% Cr(VI) removal was observed at pH 2.0 to 5.0 for both the resins at 303 K though the resin matrix are different. This is due to existence of monovalent HCrO₄⁻ as dominant species in solution. HCrO₄⁻ ion needs only one active site on the resin phase for adsorption [19]. Uptake of Cr(VI) is less at pH 1 is attributed to existence of non ionic species H₂CrO₄. At pH >5, CrO₄²⁻ is predominant Cr(VI) species which require two active sites instead of one on the resin and hence removal efficiency of Cr(VI) decreases after pH 5. In alkaline conditions OH ions compete for adsorption with CrO₄²⁻ ions decreasing removal efficiency [20,21]. The percentage removal efficiency of Cr(VI) gradually decreases beyond pH 5.5 in Tulsion A-10X (MP) as compared to Amberlyst A-21 (MP) this is may be due to hydrophilic matrix of Tulsion A-10X (MP).

3.1.3. Effect of temperature and initial concentration of Cr(VI)

The adsorption of Cr(VI) on Tulsion A-10X (MP) and Amberlyst A-21(MP) in aqueous medium is investigated at 303, 323 and 343K by varying concentration between

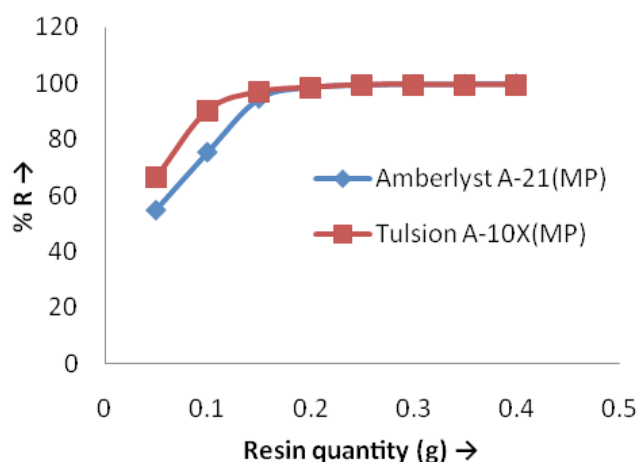


Fig. 1. Effect of resin dosage on removal of Cr(VI) on Amberlyst A-21 (MP) and Tulsion A-10X (MP).

150–450 mg·L⁻¹. At 303 K the percentage removal of Cr(VI) decreases drastically on both the resins beyond 300 mg·L⁻¹. This may be due to insufficient active sites available on the resin. According to Figs. 3, 4 and Table 2 at lower concentra-

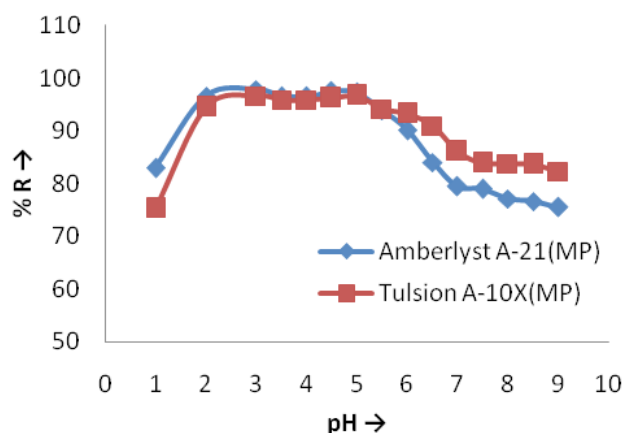


Fig. 2. Effect of pH on removal of Cr(VI) on Amberlyst A-21 (MP) and Tulsion A-10X (MP).

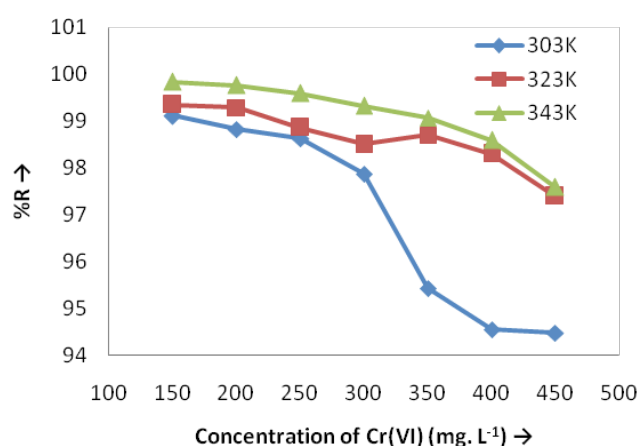


Fig. 3. Effect of initial concentration of Cr(VI) on Tulsion A-10X (MP) at 303, 323 and 343K.

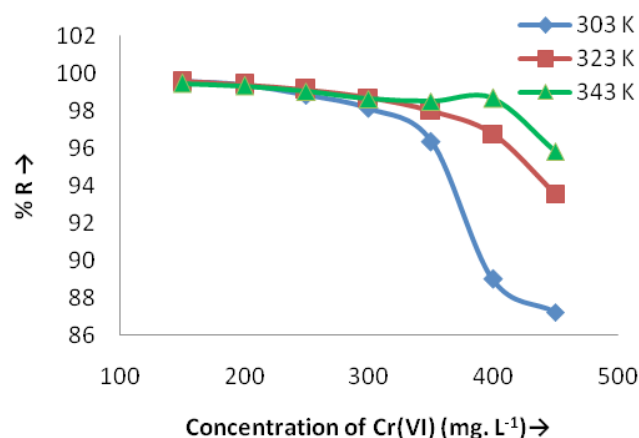


Fig. 4. Effect of initial concentration of Cr(VI) on Amberlyst A-21 (MP) at 303, 323 and 343K.

Table 2
Distribution co-efficients for adsorption of Cr(VI) on Tulsion A-10X(MP) and Amberlyst A-21(MP) in aqueous medium at 303, 323 and 343K

Resin	Temperature in K	log K_d
Tulsion A-10X (MP)	303	1.6112
	323	1.8993
	343	2.2056
Amberlyst A-21 (MP)	303	1.6322
	323	1.8389
	343	1.9128

tions 150–300 mg·L⁻¹ of Cr(VI), effect of temperature is not significant. However at higher concentrations between 350 to 450 mg·L⁻¹ of Cr(VI), the percentage removal efficiency of both the resins decreases at lower temperature. The rise in percentage removal efficiency with increase in temperature on both the resins attributed due to increase in adsorption rate. Both the resins are more effective for removal of Cr(VI) at higher temperature.

3.1.4. Effect of variation of time of contact

The study was carried out by taking 250 mg of resin and 50 cm³ Cr(VI) solution of concentration 400 mg·L⁻¹ in volumetric flask and solution is kept for shaking. The filtrate was analyzed for Cr(VI) after every 10 min time interval. In case of Tulsion A-10X(MP) the percentage removal of Cr(VI) increases with increase in contact time from 10 to 90 min but further increase has a negligible effect. Whereas for Amberlyst A-21(MP) the maximum adsorption takes place in 40 min. Fig. 5 shows the effect of variation of time of contact with concentration of Cr(VI). This indicates that adsorption is fast on polystyrene based resin than acrylic based resin.

3.1.5. Effect of addition of organic solvent on adsorption

The effect of addition of substituted ethanols like 2-methoxyethanol, 2-ethoxy-ethanol, 2-butoxyethanol on adsorption of Cr(VI) is investigated as they are frequently used as industrial solvents [22]. The adsorption of Cr(VI) decreases with increase in addition of organic solvents from 40 to 80% as shown in the Table 3. Added solvent decreases the ionization of the electrolyte in solution and reduces dielectric constants of mixed media. This indicates that Cr(VI) prefers more solution phase than resin phase at higher solvent compositions for all three solvents.

3.2. Adsorption isotherm analysis

Adsorption isotherms give the relation between the concentration of the adsorbate in the solution and on the adsorbent [23]. The equilibrium data of adsorption of Cr(VI) on the resins for three temperatures 303, 323 and 343 K was fitted in Langmuir and Freundlich isotherm models. The isotherm data is represented in Table 4.

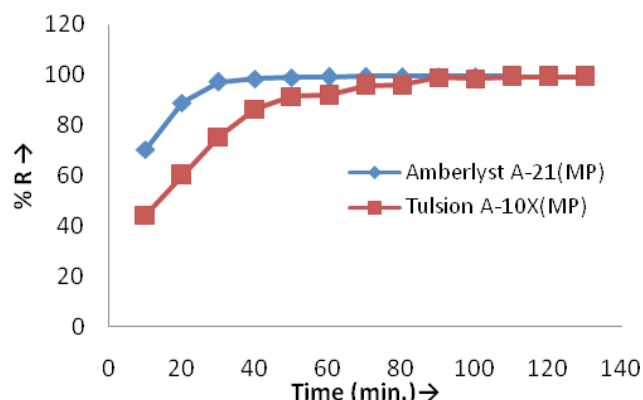


Fig. 5. Effect of variation of time of contact for adsorption of Cr(VI) on Amberlyst A-21 (MP) and Tulsion A-10X (MP).

Table 3
Distribution co-efficients for adsorption of Cr(VI) on Tulsion A-10X(MP) and Amberlyst A-21(MP) in mixed medium at 303 K

Resin	Solvent composition	log K_d		
		2-Methoxy ethanol	2-Ethoxy ethanol	2-Butoxy ethanol
Tulsion A-10X (MP)	00	1.6112	1.6112	1.6112
	40	1.1162	0.8429	1.1597
	80	0.0482	-0.0806	0.7206
Amberlyst A-21 (MP)	00	1.6322	1.6322	1.6322
	40	1.1816	0.8283	1.2680
	80	0.3796	0.2418	0.7788

3.2.1. Langmuir isotherm model

According to the linear form of Langmuir isotherm which frequently applied for monolayer processes [24] is given by Eq. (5)

$$\frac{C_e}{q_e} = \frac{1}{K_L \cdot Q_L} + \frac{C_e}{Q_L} \quad (5)$$

where K_L is the Langmuir constant related to the affinity of the bonding sites ($L \cdot mg^{-1}$) and Q_L is the maximum adsorption capacity ($mg \cdot g^{-1}$), C_e ($mg \cdot L^{-1}$) is concentration of Cr(VI) in solution at equilibrium, and q_e ($mg \cdot g^{-1}$) is the equilibrium adsorption capacity.

The separation factor R_L suggest the nature of the adsorption such as favorable, unfavorable, linear and irreversible [25] and is give by Eq. (6)

$$R_L = \frac{1}{1 + K_L \cdot C_e} \quad (6)$$

Data calculated from Figs. 6 and 7 is represented in Table 4. The R_L is greater than 0 but less than 1 for all the temperatures indicating that adsorption is favourable. R^2 value is > 0.99 for both the resins which indicates that the data fits well in the Langmuir Isotherm model and the adsorption is monolayer.

Table 4
Adsorption isotherm data for adsorption of Cr(VI) on Tulsion A-10X(MP) and Amberlyst A-21 (MP) for 303, 323 and 343K

Isotherm model	Isotherm parameters	Tulsion A-10X(MP)			Amberlyst A-21 (MP)		
Temperature (K)							
		303	323	343	303	323	343
Langmuir	K_L	0.32	0.35	1.18	0.62	0.60	0.53
	Q_L	148.41	180.51	155.07	129.92	147.52	158.73
	R_L	0.22	0.38	1.00	0.08	0.17	0.26
	R^2	0.994	0.947	0.995	0.996	0.999	0.995
Freundlich	n_F	3.18	2.29	3.53	5.18	3.68	2.84
	K_F	50.09	53.56	79.62	62.91	63.10	60.23
	R^2	0.939	0.966	0.984	0.922	0.948	0.907

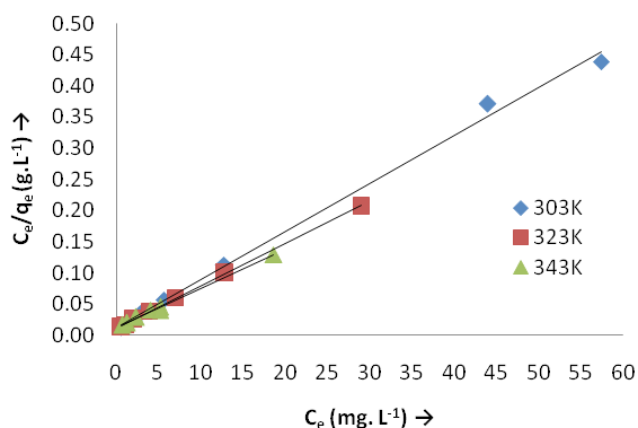


Fig. 6. Langmuir isotherm for the adsorption of Cr(VI) in aqueous medium on Amberlyst A-21(MP) at 303, 323 and 343K.

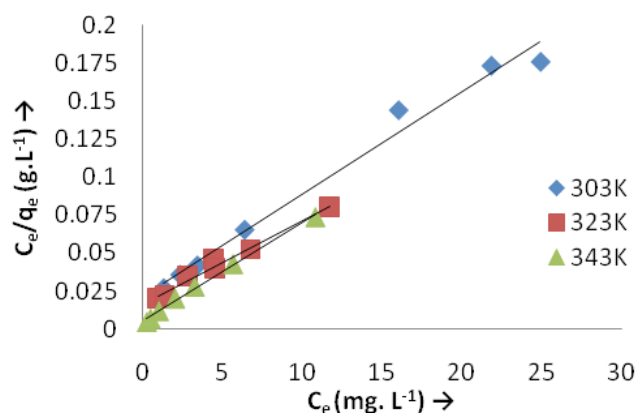


Fig. 7. Langmuir isotherm for the adsorption of Cr(VI) in aqueous medium on Tulsion A-10X(MP) at 303, 323 and 343K.

3.2.2. Freundlich isotherm model

Multilayer adsorption of adsorbate on the adsorbent is thoroughly explained by Freundlich isotherm model [26] for heterogeneous surfaces. The linear form of adsorption isotherm is given by,

$$\log q_e = \log K_F + \frac{1}{n_F} \log C_e \quad (7)$$

where K_F is Freundlich constant expressed in $\text{mg}\cdot\text{g}^{-1}$ which indicates relative adsorption capacity and n_F is the adsorption intensity.

As per the data represented in Table 4 obtained by plotting $\log q_e$ vs. $\log C_e$, the n_F values for adsorption of Cr(VI) on resins are within 1 and 10 hence the adsorption process is favourable. Increase in adsorption capacity K_F with increase in temperature confirms the endothermic nature of the adsorption process. R^2 values obtained from the isotherm for Tulsion A-10X(MP) and Amberlyst A-21(MP) are 0.939 and 0.922 respectively at 303 K. Figs. 8 and 9 represent Freundlich isotherm for the adsorption of Cr(VI) on Amberlyst A-21(MP) and Tulsion A-10X(MP) at different temperatures. Lower R^2 values for Freundlich isotherm than Langmuir isotherm indicates adsorption of Cr(VI) on the resins is monolayer.

3.3. Study of adsorption kinetics

The kinetic aspects of adsorption of Cr(VI) on Tulsion A-10X(MP) and Amberlyst A-21(MP) were studied by taking 50 cm^3 of Cr(VI) solution of $400 \text{ mg}\cdot\text{L}^{-1}$ with 250 mg of resin. The Cr(VI) concentration in the solution after adsorption was determined spectrophotometrically at different time intervals and the evolution of concentration of Cr (VI) in the solution versus time [27] is represented in Fig. 10.

The obtained experimental data was analysed for four kinetic models such as pseudo first-order, pseudo second-order, Ritchie's-second-order and the intra-particle diffusion model. The rate constants obtained for the different models together with the correlation coefficient R^2 have been listed in Table 5.

3.3.1. Lagergren's equation for first-order kinetics

The Lagergren's equation for first-order kinetics [28] is

$$\log(q_e - q_t) = \log q_e - \frac{k_1 t}{2.303} \quad (8)$$

where q_t is the amount of adsorbate adsorbed at time t in $\text{mg}\cdot\text{g}^{-1}$, k_1 is the rate constant in min^{-1} . The Lagergren's

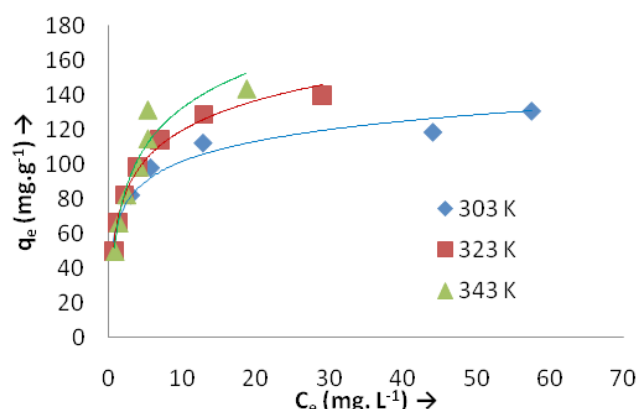


Fig. 8. Freundlich isotherm for the adsorption of Cr(VI) in aqueous medium on Amberlyst A-21(MP) at 303, 323 and 343K.

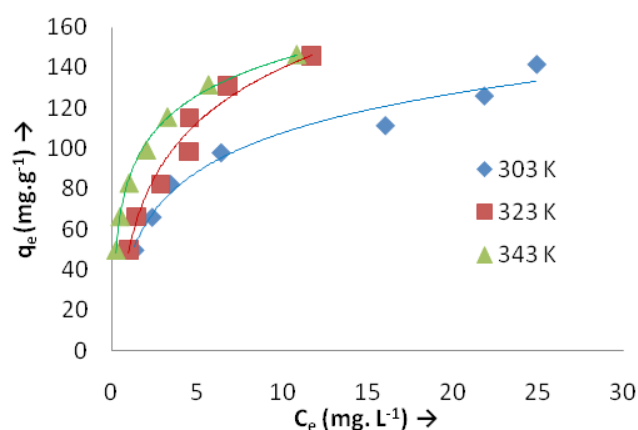


Fig. 9. Freundlich isotherm for the adsorption of Cr(VI) in aqueous media on Tulsion A 10X (MP) at 303, 323 and 343K.

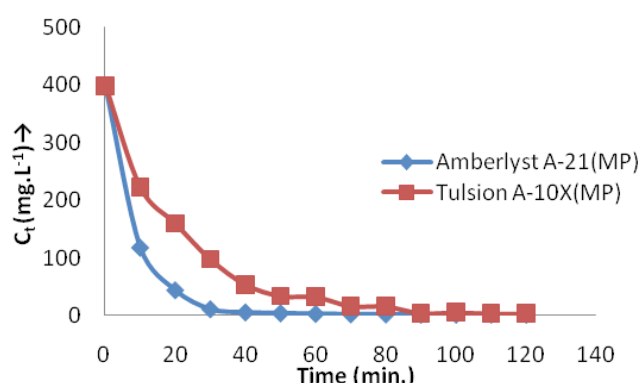


Fig. 10. Change in concentration of Cr(VI) in solution phase with time on Amberlyst A-21 (MP) and Tulsion A-10X (MP).

first-order rate constant (k_1) and q_e are calculated from the intercept and slope of the plot $\log(q_e - q_t)$ versus t as shown in Fig. 11 and the values are listed in Table 5 along with the corresponding correlation coefficients.

The correlation coefficients for the pseudo-first-order model, are relatively less i.e. 0.950 and 0.874 for Tulsion

Table 5
Kinetic parameters for adsorption of Cr(VI) on Tulsion A-10X(MP) and Amberlyst A-21 (MP)

Kinetic models	Parameters	Tulsion A-10X(MP)	Amberlyst A-21 (MP)
Pseudo-first-order kinetic model	K_1	0.0523	0.0501
	q_e	92.23	13.10
	R^2	0.950	0.874
Pseudo-second-order kinetic model	K_2	7.21×10^{-4}	4.604×10^{-3}
	q_e	91.57	82.08
	H	6.05	31.01
	R^2	0.9974	0.9993
Ritch-second order kinetic	K_R	5.22×10^2	1.52×10^3
	q_e	93.77	85.64
	R^2	0.989	0.9428
Intraparticle diffusion model	K_{id}	5.73	2.31
	a	25.71	59.29
	R^2	0.8694	0.586

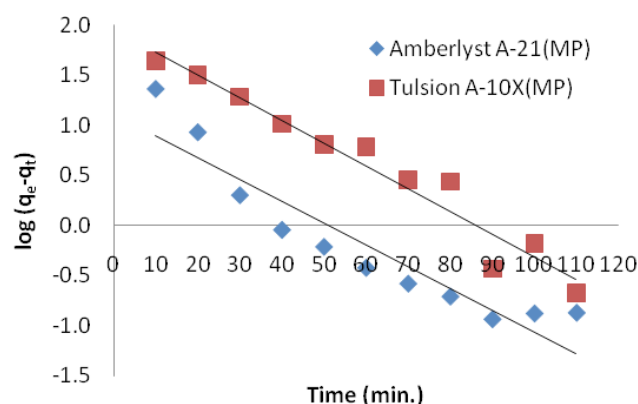


Fig. 11. Pseudo first order kinetic model for the adsorption of Cr(VI) on Amberlyst A-21(MP) and Tulsion A-10X(MP).

A-10X (MP) and Amberlyst A-21(MP) respectively. These results imply that the adsorption of Cr(VI) onto resins is not an ideal pseudo-first-order reaction.

3.3.2. Pseudo second-order model

Pseudo second-order model [29] is represented as

$$\frac{t}{q_t} = \frac{1}{k_2 q_e^2} - \frac{1}{q_e} t \quad (9)$$

where k_2 is second-order constant ($\text{g}\cdot\text{mg}^{-1}\cdot\text{min}^{-1}$) can be determined experimentally from the slope and intercept of plot t/q_t versus t as shown in Fig. 12. The k_2 and q_e calculated from the model are also listed in Table 5 along with the corresponding correlation coefficients.

For the pseudo-second-order model, the correlation coefficients are higher than 0.99 for both the resins which

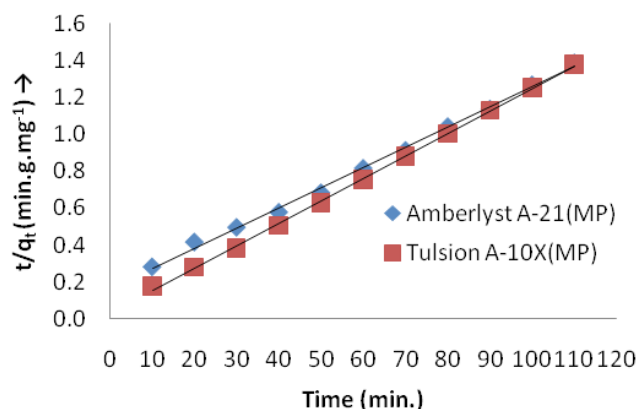


Fig. 12. Pseudo second order kinetic model for the adsorption of Cr(VI) on Amberlyst A-21(MP) and Tulsion A-10X(MP).

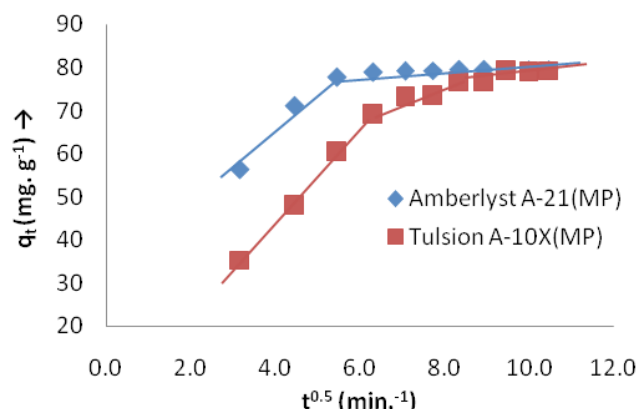


Fig. 13. Intra particle diffusion model for the adsorption of Cr(VI) on Amberlyst A-21(MP) and Tulsion A-10X(MP).

suggest that the adsorption of Cr(VI) on resins follows pseudo-second-order reaction.

3.3.3. Ritchie's second order kinetic model

The modified Ritchie's second order kinetic model [30] is represented as per Eq. (10)

$$\frac{1}{q_t} = \frac{1}{k_R q_e t} - \frac{1}{q_e} \quad (10)$$

where k_R is the rate constant (min^{-1}) of the modified Ritchie's-second-order kinetic model.

For the modified Ritchie's-second-order model, the correlation coefficients are 0.989 and 0.943 for Tulsion A-10X (MP) and Amberlyst A-21(MP) respectively, hence the adsorption of Cr(VI) on both the resins also follows modified Ritchie's-second-order kinetic model.

3.3.4. Intra-particle diffusion

The adsorption process may be controlled by either one or combination of more than one step, such as film or boundary-layer diffusion, intra-particle diffusion, surface diffusion and adsorption into the pore surface or combinations of more than one step. The intraparticle diffusion model [31] can be applied for the Cr(VI) on resins as per Eq. (11)

$$\text{AQ1} \quad q_t = k_{id} t^{0.5} + a \quad (11)$$

where k_{id} is the intraparticle rate constant in $\text{mg.g}^{-1}.\text{min}^{1/2}$ and a is gradient of linear plot. The value of ' a ' depicts rate factor i.e. the percent of adsorbate adsorbed per unit time.

The analysis of the adsorption of Cr(VI) on resins with intra-particle diffusion model Fig. 13 depicts that the adsorption process proceeds by surface diffusion at the earlier stages and by intra-particle diffusion at the later stages. The correlation coefficients (R^2) values are represented in Table 5.

3.4. Study of thermodynamic parameters

The Van't Hoff equation can be applied to study thermodynamic parameters and it is given by Eq. (12) [32].

$$\ln K_d = \frac{\Delta S^0}{R} - \frac{\Delta H^0}{RT} \quad (12)$$

The change in enthalpy ΔH^0 and change in entropy ΔS^0 of the adsorption process can be determined from the slope and intercept of plot $\ln K_d$ vs. $1/T$.

The Gibbs free energy ΔG^0 is calculated by using Eq. (13)

$$\Delta G^0 = \Delta H^0 - T\Delta S^0 \quad (13)$$

Table 6 represents thermodynamic data generated for the adsorption study, the negative ΔG^0 value indicates the adsorption of Cr(VI) on Tulsion A-10X(MP) and Amberlyst A-21 (MP) is feasible and spontaneous. The positive ΔH^0 value suggests the endothermic nature of the adsorption process. The positive ΔS^0 value indicates the increase in randomness at the solid-solute interface during the adsorption of Cr (VI).

3.5. Characterization of the resins before and after adsorption of Cr(VI)

Tulsion A-10X(MP) is a polyacrylic-co-polymer resin with polyamine groups and Amberlyst A-21(MP) is a polystyrene co-polymer resin with tertiary amine groups. Fig. 14 shows the FTIR spectra of the Amberlyst A-21(MP) resin taken before carrying out adsorption studies and the presence of spectral bands centered at around 1463 cm^{-1} confirms the presence of tertiary amine surface groups. Presence of bands at 730 , 811 and 862 cm^{-1} suggests presence of C–Cl vibrations. Two peaks at 2854 cm^{-1} and 2924 cm^{-1} indicating C–H stretching vibrations from $-\text{CH}_2$ or $-\text{CH}_3$ groups. Weak bands present between 1400 – 1450 cm^{-1} corresponds to bending vibrations of $-\text{CH}_2$ and $-\text{CH}_3$ groups.

The FTIR spectrum of resin Amberlyst A-21(MP) taken after the adsorption studies shows a band and a shoulder at 801 cm^{-1} and $1,028 \text{ cm}^{-1}$ reveals the presence of Cr–O and Cr=O bonds respectively. This confirms presence of Cr(VI) on the resin.

Table 6
Thermodynamic parameters for adsorption of Cr(VI) on Tulsion A-10X(MP) and Amberlyst A-21 (MP)

	Temperature (K)	$\ln k_d$	ΔG^0 (kJ·mol ⁻¹)	ΔH^0 (kJ·mol ⁻¹)	ΔS^0 (J·mol ⁻¹ ·K ⁻¹)
Tulsion A-10X (MP)	303	3.96	-9.76	31.92	137.59
	323	4.48	-12.52		
	343	5.45	-15.27		
Amberlyst A-21 (MP)	303	4.43	-11.23	3.13	47.39
	323	4.58	-12.18		
	343	4.58	-13.12		

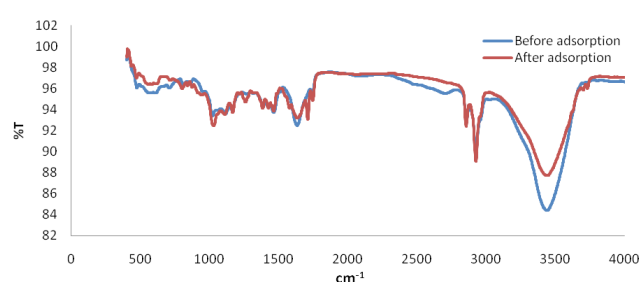


Fig. 14. FT-IR spectra of Amberlyst A-21(MP) before and after adsorption of Cr(VI).

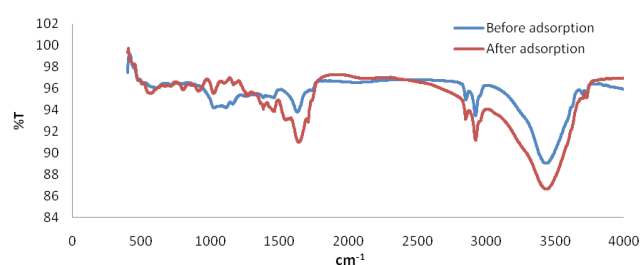


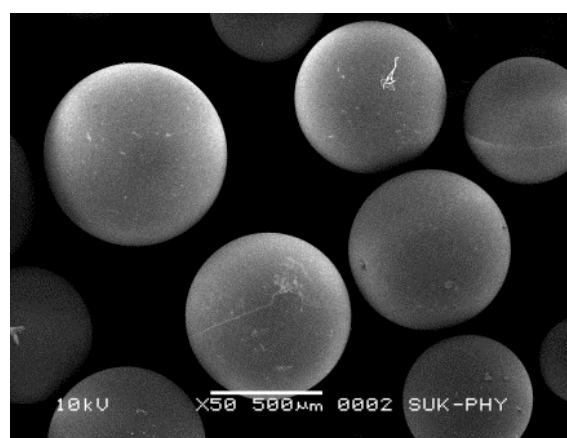
Fig. 15. FT-IR spectra of Tulsion A-10X (MP) before and after adsorption of Cr(VI).

Similarly FTIR spectrum of Tulsion A-10X(MP) before adsorption as seen in Fig. 15 shows peak at 3437 cm⁻¹ which indicates presence of hydroxyl and amine groups. The band at 2928 cm⁻¹ attributes to symmetric stretch vibrations of the -CH₂ groups. The band centered at 605 cm⁻¹ indicates presence of C-Cl bond.

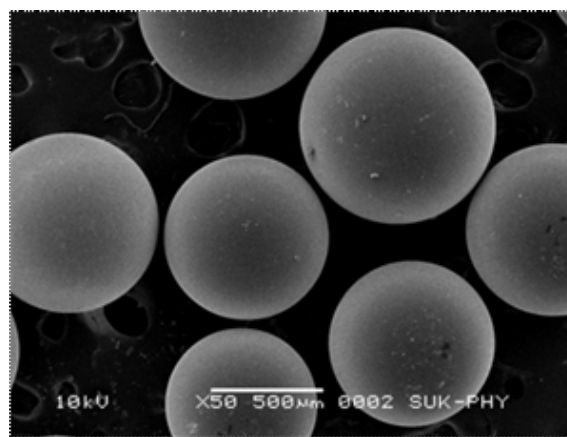
The FTIR spectrum of Tulsion A-10X(MP) taken after the adsorption studies shows a band at 803 cm⁻¹ and a shoulders at 9130, 1,020 cm⁻¹ reveal the presence of Cr-O and Cr=O bonds respectively. This confirms presence of Cr(VI) on the resin.

3.6. Scanning electron microscopy of the resins

Scanning electron microscopy (SEM) images taken before and after adsorption of Cr(VI) on resins Tulsion A-10X(MP) and Amberlyst A-21(MP) are depicted in the Figs. 16(a), 16(b), 17(a) and 17(b). There is no change in surface morphology of resin after the adsorption for Cr(VI) which indicates the stability of the resins with acrylic and



Before adsorption (a)



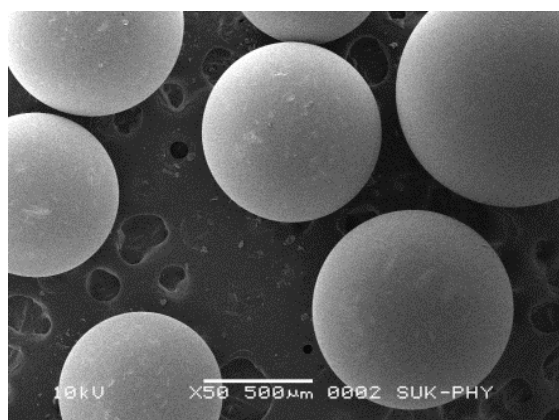
After adsorption (b)

Fig. 16. SEM Images of Tulsion A-10X(MP).

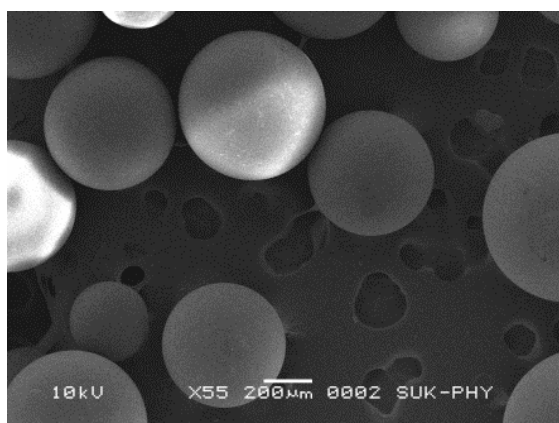
polystyrene matrix. This suggests that removal of Cr(VI) is possible by using both the resins up to 343 K without change in resin morphology.

3.7. Desorption studies

Desorption study indicates that NaOH is more efficient desorbent than HCl and EDTA. Fig. 18 represents



Before adsorption (a)



After adsorption (b)

Fig. 17. SEM Images of Amberlyst A-21(MP).

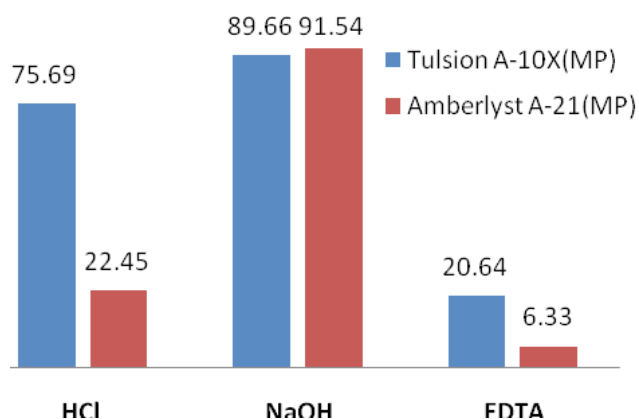


Fig. 18. Desorption of Cr(VI) on Tulstion A-10X(MP) and Amberlyst A-21(MP) by using different desorbents.

the percentage of Cr(VI) desorbed after treatment with desorbents. However, for the recovery of Cr(VI) as Chromic acid (H_2CrO_4) from the resin, HCl is useful desorbent. Chromic acid recovery is more in case of Tulstion A-10X(MP) than in case of Amberlyst A-21(MP). From the desorption studies using various desorbents we can

conclude that Tulstion A-10X(MP) with acrylic matrix is more useful for Cr(VI) removal and recovery of Cr(VI) as chromic acid from chrome plating drag out and rinse water.

4. Conclusion

On the basis of the results obtained from the adsorption studies of Cr(VI) on weak base resins in aqueous and mixed media we can conclude that Cr(VI) removal efficiency is highest in the pH range of 3–6 and increases with the increase in resin dosage and temperature. The presence of solvent in the external phase influences adsorption of Cr(VI) on the resins studied and it decreases with increase in solvent compositions. The equilibrium data fits in well with Langmuir isotherm, which indicates monolayer adsorption of Cr(VI) on both the resins. The kinetic studies for removal of Cr(VI) on both the resins follow the pseudo-second order kinetic model, controlled by film diffusion in the initial stage and intraparticle diffusion in the later stage. The desorption study indicates that though NaOH is more appropriate desorbent for both the resins but for the recovery of Cr(VI) as chromic acid HCl is more efficient desorbent on Tulstion A-10X(MP). Hence, Tulstion A-10X(MP) is suitable for removal and recovery of Cr(VI) from chrome plating drag out and rinse water at various temperatures due to better stability of the resin. However adsorption and regeneration of Cr(VI) is more rapid on Amberlyst A-21(MP) having styrene divinyl benzene resin matrix.

Acknowledgement

Authors would like to thank Thermax Limited, Pune, India for providing free samples of the resin for the research work.

References

- [1] M.C. Golonka, Toxic and mutagenic effects of chromium (VI): a review, *Polyhedron*, 15 (1996) 3667–3675.
- [2] S. Bajpai, G. Jung, A. Dey, Batch studies on chromium removal from tannery effluent using cationic exchange resin, *J. Environ. Res. Develop.*, 4 (2009) 77–82.
- [3] K. Dermentzis, A. Christoforidis, E. Valsamidou, A. Lazaridou, N. Kokkinos, Removal of hexavalent chromium from electroplating wastewater by electrocoagulation with iron electrodes, *Global NEST J.*, 13 (2011) 412–418.
- [4] S. Parlayıcı, A. Yar, A. Avci, E. Pehlivan, Removal of hexavalent chromium using polyacrylonitrile/titanium dioxide nanofiber membrane, *Desal. Water. Treat.*, 57 (2016) 16177–16183.
- [5] M. Rajasimman, R. Sangeetha, P. Karthik, Statistical optimization of process parameters for the extraction of chromium(VI) from pharmaceutical wastewater by emulsion liquid membrane, *Chem. Eng. J.*, 150 (2009) 275–279.
- [6] R. Gayathri, P. Senthil Kumar, Recovery and reuse of hexavalent chromium from aqueous solutions by a hybrid technique of electro dialysis and ion exchange, *Braz. J. Chem. Eng.*, 27 (2010) 71–78.
- [7] Y. Xing, X. Chen, P. Yao, D. Wang, Continuous electrode ionization for removal and recovery of Cr(VI) from wastewater, *Sep. Purif. Technol.*, 67 (2009) 123–126.
- [8] K. Mubeena, G. Muthuraman, Extraction and stripping of Cr(VI) from aqueous solution by solvent extraction, *Desal. Water. Treat.*, 55 (2014) 2201–2208.

- [9] E. Malkoc, Y. Nuhoglu, M. Dundar, Adsorption of chromium (VI) on pomace - an olive oil industry waste: batch and column studies, *J. Hazard. Mater.*, B138 (2006) 142–151.
- [10] L. Rafati, A.H. Mahvi, A.R. Asgari, S.S. Hosseini, Removal of chromium (VI) from aqueous solutions using Lewatit FO36 nano ion exchange resin, *Int. J. Environ. Sci. Tech.*, 7 (2010) 147–156.
- [11] E. Korngold, N. Belayev, L. Aronov, Removal of chromates from drinking water by anion exchangers, *Sep. Purif. Technol.*, 33 (2003) 179–187.
- [12] E. Pehlivan, S. Cetin, Sorption of Cr(VI) ions on two Lewatit-anion exchange resins and their quantitative determination using UV-visible spectrophotometer, *J. Hazard. Mater.*, 163 (2009) 448–453.
- [13] G. Wojcik, V. Neagu, I. Bunia, Sorption studies of chromium(VI) onto new ion exchanger with tertiary amine, quaternary ammonium and ketone groups, *J. Hazard. Mater.*, 190 (2011) 544–552.
- [14] J. Rashid, M.A. Barakat, M.A. Alghamdi, Adsorption of Chromium (VI) from wastewater by anion exchange resin, *J. Adv. Catal. Sci. Technol.*, 1 (2014) 26–34.
- [15] C. Balan, I. Volf, D. Bilba, Chromium (VI) removal from aqueous solutions by purolite base anion-exchange resins with gel structure, *Chem. Ind. Chem. Eng. Q.*, 19 (2013) 615–628.
- [16] Method 7196A: Chromium Hexavalent (Colorimetric), SW-846 third ed., United States Environmental Protection Agency, Washington DC, 1992.
- [17] E. Pehlivan, T. Altun, Ion-exchange of Pb^{2+} , Cu^{2+} , Zn^{2+} , Cd^{2+} and Ni^{2+} ions from aqueous solution by Lewatit CNP 80, *J. Hazard. Mater.*, 140 (2007) 299–307.
- [18] A.A. Atia, Synthesis of a quaternary amine anion exchange resin and study its adsorption behaviour for chromate oxyanions, *J. Hazard. Mater.*, B137 (2006) 1049–1055.
- [19] X. Liu, Y. Li, C. Wang, M. Ji, Comparison study on Cr(VI) removal by anion exchange resins of Amberlite IRA96, D301R, and DEX-Cr: isotherm, kinetics, thermodynamics and regeneration studies, *Desal. Water Treat.*, 55 (2015) 1840–1850.
- [20] P.S. Koujalagi, S.V. Divekar, R.M. Kulkarni, E.M. Cuerda-Correa, Sorption of hexavalent chromium from water and water-organic solvents onto an ion exchanger Tulsion A-23(Gel), *Desal. Water Treat.*, 57 (2016) 23965–23974.
- [21] M.R. Gandhi, N. Viswanathan, S. Meenakshi, Adsorption mechanism of hexavalent chromium removal using Amberlite IRA 743 resin, *Ion Exch. Lett.*, 3 (2010) 25–35.
- [22] M. Dieter, NTP technical report on the toxicity studies of ethylene glycol ethers: 2-methoxyethanol, 2-ethoxyethanol, 2-butoxyethanol (CAS Nos. 109-86-4, 110-80-5, 111-76-2) administered in drinking water to F344/N rats and B6C3F1 mice, *Toxic Rep. Ser.*, 26 (1993) 1-G15.
- [23] H. Zheng, D. Liu, Y. Zheng, S. Liang, Z. Liu, Sorption isotherm and kinetic modeling of aniline on Cr-bentonite, *J. Hazard. Mater.*, 167 (2009) 141–147.
- [24] A. Kara, E. Demirbel, Kinetic, isotherm and thermodynamic analysis on adsorption of Cr(VI) ions from aqueous solutions by synthesis and characterization of magnetic-poly(divinylbenzene-vinylimidazole) microbeads, *Water Air Soil Pollut.*, 223 (2012) 2387–2403.
- [25] K. Kadirvelu, K. Thamaraiselvi, C. Namasivayam, Adsorption of nickel (II) from aqueous solution onto activated carbon prepared from coirpith, *Sep. Purif. Technol.*, 24 (2001) 497–505.
- [26] Y.S. Ho, D.A. John Wase, C.F. Forster, Batch nickel removal from aqueous solution by sphagnum moss peat, *Water Res.*, 29 (1995) 1327–1332.
- [27] A.E. Rodrigues, C.M. Silva, What's wrong with Lagergreen pseudo first order model for adsorption kinetics?, *Chem. Engng. J.*, 306 (2016) 1138–1142.
- [28] X.J. Hu, J.S. Wang, Y.G. Liu, X. Li, G.M. Zeng, Z.L. Bao, X.X. Zeng, A.W. Chen, F. Long, Adsorption of chromium (VI) by ethylene diamine-modified cross-linked magnetic chitosan resin: isotherms, kinetics and thermodynamics, *J. Hazard. Mater.*, 185 (2011) 306–314.
- [29] O. Kusku, B.L. Rivas, B.F. Urbano, M. Arda, N. Kabay, M. Bryjak, A comparative study of removal of Cr(VI) by ion exchange resins bearing quaternary ammonium groups, *J. Chem. Technol. Biotechnol.*, 89 (2014) 851–857.
- [30] A.G. Ritchie, Alternative to Elovich equation for kinetics of adsorption of gases on solids, *J. Chem. Soc. Faraday Trans.*, 73 (1977) 1650–1653.
- [31] N. Dizge, E. Demirbas, M. Kobya, Removal of thiocyanate from aqueous solutions by ion exchange, *J. Hazard. Mater.*, 166 (2009) 1367–1376.
- [32] B. Singha, S.K. Das, Biosorption of Cr (VI) ions from aqueous solutions: kinetics, equilibrium, thermodynamics and desorption studies, *Colloids Surf. B. Biointerfaces*, 84 (2011) 221–232.